

Non-linear tendon fatigue life under uncertainties

Original

Non-linear tendon fatigue life under uncertainties / Rodriguez Reinoso, M., Antonaci, P., Pugno, N.M., Surace, C.. - In: INTERNATIONAL JOURNAL OF NON-LINEAR MECHANICS. - ISSN 0020-7462. - 163:(2024), pp. 1-11.
[10.1016/j.ijnonlinmec.2024.104751]

Availability:

This version is available at: 11583/2993496 since: 2024-10-31T09:38:58Z

Publisher:

Elsevier

Published

DOI:10.1016/j.ijnonlinmec.2024.104751

Terms of use:

This article is made available under terms and conditions as specified in the corresponding bibliographic description in the repository

Publisher copyright

Elsevier postprint/Author's Accepted Manuscript

© 2024. This manuscript version is made available under the CC-BY-NC-ND 4.0 license
<http://creativecommons.org/licenses/by-nc-nd/4.0/>. The final authenticated version is available online at:
<http://dx.doi.org/10.1016/j.ijnonlinmec.2024.104751>

(Article begins on next page)

1 Non-linear Tendon Fatigue Life under Uncertainties

2 Mariana Rodriguez Reinoso ^{a,b}, Paola Antonaci ^{a,b}, Nicola M. Pugno^{c,d}, Cecilia Surace ^{a,b}

3
4 ^a Laboratory of bioinspired Nanomechanics, Politecnico di Torino, Italy.

5 ^b Department of Structural, Geotechnical and Building Engineering, Politecnico di Torino, Italy.

6 ^c Laboratory for Bioinspired, Bionic, Nano, Meta, Materials & Mechanics, Department of Civil,
7 Environmental and Mechanical Engineering, University of Trento, Via Mesiano 77, 38123 Trento, Italy

8 ^d School of Engineering and Materials Science, Queen Mary University of London, Mile End Road, E1 4NS,
9 London, United Kingdom

10

11 **Keywords:** Tendon fatigue life, Generalised Paris Erdogan equation, Monte Carlo
12 analysis, Self healing.

13 **Abstract:** *Tendons play a pivotal role in facilitating joint movement by transmitting muscular*
14 *forces to bones. The intricate hierarchical structure and diverse material composition of tendons*
15 *contribute to their non-linear mechanical response. However, comprehensively grasping their*
16 *mechanical properties poses a challenge due to inherent variability in biological tissues. This*
17 *necessitates a thorough examination of uncertainties associated with properties measurements,*
18 *particularly under diverse loading conditions. Given the cyclic loading experienced by tendons*
19 *throughout an individual's lifespan, understanding their mechanical behaviour under such*
20 *circumstances becomes crucial.*

21 *This study addresses this need by introducing a generalised Paris Erdogan Law tailored for non-*
22 *linear materials. To examine uncertainties within this proposed framework, Monte Carlo*
23 *Analysis is employed. This approach allows for a thorough exploration of the uncertainties*
24 *associated with tendon mechanics, contributing to a more robust comprehension of their*
25 *behaviour under cyclic loading conditions.*

26 *Finally, self-healing has been integrated into the fatigue law of tendons through the proposal of*
27 *a healing function, formulated as a polynomial function of the maximum stress. This approach*
28 *allows to account for an increase in the number of cycles for each stress value due to self-repair*
29 *after the damage event generated by long-term cycling load over the individual's life span.*

30 1. Introduction

31 Tendons are connective tissues that play a crucial role on joint movements, since they
32 enable to transfer the forces developed by muscles to the bones thus allowing locomotion
33 [1]. Due to their high tensile strength, tendons efficiently transmit bursting forces much
34 like springs, while also providing the flexibility necessary for a wide range of joint
35 motions. Their structure allows to perform this role in such an efficient way, that they
36 have a damping effect during the initial part of muscles force transmission and during
37 high impact loading, while allowing at the same time an instantaneous strain transfer
38 during movements [2], [3]. In other words, tendon compliance is able to decrease the
39 cost of muscular contraction by reducing the contractile velocity and length change for a
40 given movement while boosting the power output of muscle-tendon units [4].

41 Tendons normally are subject to high levels of in vivo stresses [5]; they undergo small
42 repetitive strains that cause microinjuries that gradually accumulate [6], [7]. As a result,

43 tendons are prone to present some overuse injuries which are collectively referred to as
44 tendinopathy. The latter is related to a poor healing response, with tenocyte
45 degeneration and random proliferation, collagen fibre disruption, and an increase in
46 non-collagenous matrix [8], [9]. In literature different studies have shown that low levels
47 of post operative active forces applied to the repair site in the immediate postoperative
48 period improve the tendon healing efficiency, and the application of excessive stress to
49 an immature repair site would lead to a gap formation and poor clinical results[10], [11]
50 For a comprehensive understanding of the mechanism of tendon overuse and therefore
51 their fatigue damage progression towards tendinopathy or rupture, several authors have
52 performed experimental analysis on animal tendons due to their wide availability,
53 considering in vivo and ex vivo experimental methods [12]. Among the ex vivo
54 experimental tests, Wang et al.[13] and Ker et al.[14] analysed cycling loading of Wallaby
55 tail tendons, Pedaprolu et al. analysed rat Achilles tendons [15], Fung et al. analysed rat
56 flexor digitorum longus [16], other studies such as Soslowsky et al.[17] and Scott et
57 al.[18] analysed rats supraspinatus tendons. Among the in vivo experimental test, Fung
58 et al.[19] and Andarawis et al.[20] analysed rat patellar tendons under cycling loading,
59 Sereysky et al.[21] analysed murine patellar tendons. Experimental data on fatigue tests
60 in human soft tissues are extremely important to improve the knowledge in this field,
61 however only few authors report human tendon data in the current scientific literature.
62 Schetchman et al. report the fatigue behaviour of 90 specimens of Human Extensor
63 Digitorum Longus (EDL) tendons evaluating nine different stress levels [22], Wren et al.
64 report the fatigue behaviour under cycling loading for 25 specimens for human Achilles
65 tendon[23]. Firminger et al. report the fatigue behaviour of 30 specimens of Human
66 patellar tendon [24].

67 Soft tissues typically present non-linear mechanical response. More precisely, the
68 mechanical behaviour of tendons is viscoelastic, thus, their load-displacement
69 relationships are rate-dependent and history-dependent. A typical viscoelastic J- shaped
70 stress-strain curve for tendon shows three different regions: a toe region for low stress
71 due to tendon compliance (the stretch increases significantly as the load increases), a
72 linear region at greater stresses and strains where the tendon stiffness increases up to
73 reaching a fairly uniform elastic modulus, and finally a failure zone [16], [19], [25], [26],
74 [27]. Typically, the linear region is predominant with respect to the others, indeed
75 during a hysteresis loop, the tendon returns up to 90-95% of the stored energy and
76 dissipate about 5-10%[4]. In addition, the mechanical behaviour of soft tissues normally
77 presents a high degree of variability, due to internal and external factors. Indeed, the

78 results of ex-vivo tests may vary according to the specimen, the location of harvesting,
79 the conservation method, the experimental setup and measuring of the specimens.
80 Therefore, even if an accurate mechanical model can be formulated, the model may not
81 necessarily be adequate to predict the behaviour of another specimen. Since it is
82 impossible to achieve a full knowledge of the all the parameters of the mechanical model,
83 some assumptions are needed, and this introduces uncertainties into the results.

84 Over the time, few authors have developed fibrous soft tissues fatigue models with the
85 aim to predict the number of cycles for fatigue failure[28], [29], [30], [31]. In particular,
86 Bosia et al. developed a model for fatigue of self-healing soft nanomaterial as tendons
87 [30], Adeeb et al. applied the notions of Linear Fracture Mechanics for the development
88 of fatigue behaviour of tendon models [31]. In both studies, the authors considered the
89 Paris law for fatigue damage propagation as the starting point for their models: due to
90 its robustness and suitability for multiple applications to different materials, the authors
91 convey that this fatigue damage propagation law should be appropriate also for tendons
92 and ligaments. However, the use of the Paris Law to describe the crack propagation in a
93 non-linear material might be a restrictive approach that does not capture the innate non-
94 linear mechanical behaviour of tendons.

95 In this context, it may be difficult to give an accurate prediction of the level of damage
96 within a biological structure, because of the random variations and extremely high
97 variability in terms of geometry and other mechanical features of the specimens. This
98 suggests that also their lifetime will be a random variable likewise. Given the uncertain
99 nature of the parameters, it might be useful to obtain boundaries for the estimation of
100 the lifetime of the structure under study.

101 The analysis of uncertainties on the constitutive modelling for soft tissues is still in early
102 stage. A recent study developed by Hosseini Nasab et al. analysed the accuracy of the
103 estimation of the contact force due to the uncertainties in the parameters related to the
104 muscle-tendon system by a probabilistic approach [32]. A study by Balzani et al.
105 proposed a computational method for the assessment of rupture probabilities in soft
106 collagenous tissues [33]. Another study of Haughton et al. proposed a new
107 microstructural hyperelastic model for the mechanical behaviour of tendons, and to
108 account for the parameters uncertainties they employed the Markov chain Monte Carlo
109 algorithm [34]. In this context, Montecarlo Method can be employed to investigate the
110 propagation of uncertainty on the lifetime prediction, and it appears to be one of the
111 most suitable methods for modelling complex systems with multiple variables and
112 uncertainties [34], [35], [36].

113 The main objectives of this paper are: i) the development of a Generalised Paris-Erdogan
114 (GPE) law for non-linear materials, and ii) the analysis of the uncertainties that
115 encompass the tendon fatigue mechanical behaviour by using Monte Carlo (MC)
116 method. The GPE law here proposed will be developed considering some of the
117 principles used by Carpinteri et al. for the fracture behaviour of Functionally Graded
118 Materials (FGMs) [37], in which the stress intensity factor, rather than being a constant,
119 varies with the structural size, the nominal strength and the fracture toughness of the
120 material. Other principles employed by Pugno et al. regarding Atomistic Fracture [38]
121 will also be included. The parameters for the proposed GPE will be obtained by
122 integration within a genetic algorithm that performs data fitting between experimental
123 data and the number of cycles obtained by integration for each stress value. In this study
124 an experimental dataset for EDL tendons will be considered [22].

125 Furthermore, following a similar approach for the introduction of self-healing effect by
126 Bosia et al. [29] an additional analysis will be performed considering the introduction of
127 the healing rate within the GPE approach here proposed. The healing effect will be
128 considered as a function of other parameters rather than a constant, as suggested in [29].
129 In particular, it will be introduced as a function of the maximum stress applied on the
130 tendon, assuming that, for a given healing rate value η , it increases up to a critical stress
131 value. Subsequently, the healing rate value starts to decrease due to the formation of the
132 gap.

133 The paper is structured as follows: in section 2 the development of the GPE law is
134 explained; in Section 3 the numerical approach for GPE integration is presented; In
135 section 4 the method for the introduction of the Healing Function (HF) is shown; In
136 section 5 the Monte Carlo analysis is described; in section 6 the results are shown and
137 discussed.

138 2. Development of the Generalised Paris Erdogan law for non-linear materials.

139 2.1. Linear elastic fracture mechanics principles and fatigue life.

140 According to Linear Elastic Fracture Mechanics principles, for a rectangular plate of
141 finite dimensions, with a mode I crack subjected to uniaxial tension, the stress intensity
142 factor (SIF) denoted as K_I regulates the amplification of the applied stress σ in the field
143 near to the crack tip. The SIF is expressed as shown in equation 1, where: Y is a function
144 that depends on the crack and loading geometries; $2a$ represents the crack's width. In
145 the case of a finite plate with a central crack, the value of the function Y is reported in
146 equation 2, where $2b$ denotes the plate's width.

$$K_I = Y\sigma\sqrt{\pi a} \quad (1)$$

$$Y = \sqrt{\sec\left(\frac{\pi a}{2b}\right)} \quad (2)$$

147 The critical energy release rate J_c , is a mechanical property that describes the ability of
 148 a material to resist the propagation of cracks. It is normally determined by making an initial
 149 notch, or crack, in the material and measuring the energy required to create a determined
 150 amount of new crack area [39], [40]. According to Linear Elastic Fracture Mechanics, for
 151 the case of an isotropic linear elastic material there is a relationship between the failure
 152 stress σ_f and the half crack length a , as reported in Equation 3 (where E is the Elastic
 153 Modulus of the material and Y is a function of the crack and loading geometries). The
 154 parameter $(J_c E)^{1/2}$ is known as the Critical Stress Intensity Factor K_{Ic} .

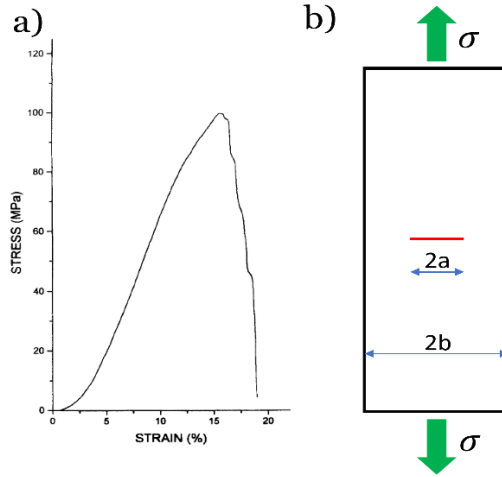
$$K_{Ic} = \sqrt{J_c E} = Y\sigma_f\sqrt{\pi a} \quad (3)$$

155 The Paris-Erdogan law is an empirical model that describes the progressive growth of
 156 a crack under cycling loading conditions in linear elastic materials. It expresses a power
 157 relationship between the rate of the crack growth with respect to the number of cycles,
 158 da/dN , and the difference $\Delta\sigma$ between the maximum and the minimum stress levels applied
 159 during the cyclic loading: $\Delta\sigma = \sigma_{max} - \sigma_{min}$. It is shown in equation 4, where C and m_p are
 160 the Paris constants, that can be determined experimentally [30].

$$\frac{da}{dN} = C(Y\Delta\sigma\sqrt{\pi a})^{m_p} = C(\Delta K_I)^{m_p} \quad (4)$$

161 2.2. Generalised Paris -Erdogan law for non-linear materials

162 Tendons exhibit non-linear mechanical behaviour, as already mentioned in Section 1.
 163 Figure 1a illustrates a typical stress-strain curve for Human Extensor Digitorum Longus
 164 (EDL) tendons, reproduced from the work of Schechtman et al. [22]. The curve displays a
 165 typical viscoelastic J-shaped profile, characterised by three distinct regions: a toe region
 166 for low stress; a linear region at higher stresses and strains, where the tendon stiffness
 167 increases to achieve a fairly uniform elastic modulus; and finally, a failure zone.



168

169

170

Figure 1. a) A Typical Stress- Strain Curve for EDL tendons from Schechtman et al [22], b) Tendon modelled as a slender rectangular plate, subjected to uniaxial tension, with a Type 1 crack located in the centre of the plate.

171

172

173

174

175

176

177

178

In this context, the traditional Paris-Erdogan law may not be the most suitable model to describe the crack growth under cyclic loading, due to material non-linearity. Therefore, in the following a generalised Paris-Erdogan law is proposed for non-linear materials. The tendon specimen under consideration can be modelled as a slender rectangular plate of finite dimensions, subjected to uniaxial tension. As in the previous section, it is hypothesised that the specific damage being examined involves a central fatigue crack exhibiting mode I opening, with the crack length extending perpendicularly to the loading axis. The crack's width is represented by $2a$, while the plate's width is denoted by $2b$, as shown in Figure 1b.

179

180

181

182

183

184

According to [38], equation 1 can be generalised for non-linear elastic materials, as shown in Equation 5, where the stress-strain constitutive law is expressed as $\sigma \propto \varepsilon^k$. Here k is a constant, and if $k > 1$ it implies hyper-elasticity, if $k < 1$ it implies elasto-plasticity, while if $k = 1$ it implies linear elasticity [38]. Equation 6 delineates the range of the stress intensity factor. The parameter α represents the power stress-singularity, modified from the classical value of $1/2$, being $\alpha = k/(k + 1)$ [41].

$$K_{NL} = Y\sigma(\pi a)^\alpha b^{\left(\frac{1}{2}-\alpha\right)} \quad (5)$$

$$\Delta K_{NL} = Y\Delta\sigma(\pi a)^\alpha b^{\left(\frac{1}{2}-\alpha\right)} \quad (6)$$

185

186

Introducing equation 6 in equation 4 the following equation is obtained:

$$\frac{da}{dN} = C \left(Y\Delta\sigma(\pi a)^\alpha b^{\left(\frac{1}{2}-\alpha\right)} \right)^{m_p} \quad (7)$$

187 Defining the generalised stress intensity factor $K_{NL}^* = Y\sigma(\pi a)^\alpha$ and the generalised
 188 SIF range $\Delta K_{NL}^* = Y\Delta\sigma(\pi a)^\alpha$, equation 8 is obtained.

$$\frac{da}{dN} = C \left(\Delta K_{NL}^* b^{\left(\frac{1}{2}-\alpha\right)} \right)^{m_p} \quad (8)$$

189 Designating $C_{NL}^* = C \left(b^{\left(\frac{1}{2}-\alpha\right)} \right)^{m_p}$ equation 4 can be written as:

$$\frac{da}{dN} = C_{NL}^* (\Delta K_{NL}^*)^{m_p} \quad (9)$$

190 According to the work of Carpinteri and Pugno [37] it is possible to define a generalised
 191 critical stress intensity factor as follows, where UTS is the ultimate tensile strength:

$$K_{IC}^* = (1 - \alpha)UTS \left(\frac{2K_{IC}}{UTS} \right)^{2\alpha} \quad (10)$$

192 During cyclic loading, the crack length will consistently increase. The criterion for
 193 terminating the process is determined by reaching the point at which the tendon specimen
 194 fails, marked by the generalised SIF reaching the critical generalised SIF K_{IC}^* . This threshold
 195 can be considered a critical value beyond which the material succumbs to fracture.

196 3. Numerical approach for GPE integration.

197 3.1. Experimental data collection

198 The experimental data were collected from a study of Schechtman et al. in which the
 199 authors analysed the fatigue behaviour of ninety specimens of Human Extensor Digitorum
 200 Lungus (EDL) tendons under square cycling loading with minimum stress level almost
 201 equal to zero and a maximum stress level in the range 10% – 90% of the Ultimate Tensile
 202 Strength UTS (100 MPa), and a frequency loading (1, 2, 3, 4 Hz) that changed according to
 203 the stress level that was applied [22].

204 3.2. Integration of the Generalised Paris- Erdogan law for non-linear materials

205 In this section, the GPE law for non-linear materials (equation 9) is integrated
 206 employing a forward Euler method. In particular, the GPE law has been considered written
 207 in its inverse form as shown in equation 11. The integration requires determining the most
 208 suitable values for the material constants K_{IC} , C and m_p , which play a crucial role on the
 209 description of the material behaviour during cycling loading, and therefore the rate of the
 210 crack growth with respect to the number of cycles. A Genetic Algorithm (GA) is employed to

211 perform the optimisation of this constants within the MATLAB environment, allowing to
 212 find the values $m_{bestfit}$, $C_{bestfit}$ and $K_{IC\ bestfit}$. The objective function f chosen to minimise
 213 with the GA algorithm is a sum of two terms. The first term $E1$ represents the sum of the
 214 relative error with respect to the number of cycles obtained by fitting N_{fit} , while the second
 215 term $E2$ pertains to the sum of the relative errors with respect to the experimental number
 216 of cycles, N_{exp} .

$$\frac{dN}{da} = (C_{NL}^* (\Delta K_{NL}^*)^{m_p})^{-1} \quad (11)$$

$$E1 = \sum abs\left(\frac{N_{exp} - N_{fit}}{N_{fit}}\right) \quad (12)$$

$$E2 = \sum abs\left(\frac{N_{exp} - N_{fit}}{N_{exp}}\right) \quad (13)$$

$$f = E1 + E2 \quad (14)$$

217 The parameters set for the integration were as follows: the initial half-crack width $a_0 =$
 218 $b/6$, with $b = 1.5$ mm representing the tendon's half-width; the ultimate tensile strength
 219 $UTS = 100$ MPa. The power of the stress singularity α was determined based on the work by
 220 Bosia et al., where $k = 2.33$, resulting in $\alpha = 0.7$ [30]. The values chosen for the search space
 221 are outlined in Table 1. The boundaries for the critical SIF K_{IC} were selected to encompass
 222 values found in the literature for other biological tissues [40]. Meanwhile, the values for the
 223 dimensionless constant m_p in the Paris-Erdogan law were set based on the various values
 224 obtained in the work of Adeeb et al. for EDL tendons [31]. Regarding parameter C , due to a
 225 lack of available literature data on its specific value for biological soft tissues, its boundaries
 226 have been determined after conducting some preliminary GA parameter optimisations.
 227 These boundaries encompass the entire range of values obtained during the optimisation
 228 process.

229

Table 1: Values for the upper and lower research boundaries with their respective units in square brackets.

230

231

232

Variable	min	max
m_p	4	6
C [MPa $^{-m_p}$ m $^{m_p/2+1}$]	10^{-7}	10^{-5}
K_{IC} [MPa \sqrt{m}]	3	6

233

4. Introduction of the healing rate

234

235

236

237

238

239

240

241

242

243

244

245

246

247

Self-healing and remodelling processes occur within in vivo tissues, enabling them to heal microtraumas caused by repetitive or more extreme activities and stresses such as normal walking or sporting. However, all literature on the fatigue life of human tendons has been obtained using in vitro experimental tests, resulting in an underestimation of in vivo tendon fatigue life [30]. Drawing from ex vivo tendon mechanical properties and incorporating the self-healing effect, this section proposes a fatigue life model that may accurately estimate tendon fatigue life in vivo. A previous work of Bosia et al. introduced the concept of self-healing effect on the damage equation for tendons by considering the healing rate η . Healing effect is a function of time and damage level. The authors hypothesised that being the loading slow enough, the effect of time can be neglected and therefore only the dependence on the damage level is significant. As a first approximation, the authors assumed that η is a constant and that the term of the initial crack size a_i can be modified to $a_i (1 - \eta)$. The healing rate value η can assume values from 0 to 1, being $\eta = 0$ the case in which there is no self-healing effect [30].

248

249

250

251

252

253

254

255

256

257

To the authors' best knowledge, self-healing is strongly dependent on the load that the tendon undergoes [30]. Several authors affirm that low levels of post operative active forces applied to the repair site in the immediate postoperative period improve the tendon healing efficiency, and the application of excessive stress to an immature repair site would lead to a gap formation and poor clinical results [10], [11]. On the light of this, in this study the self-healing effect will be considered within the GPE approach with $\alpha = 0.7$, by modifying the expression of the crack size a to $a(1 - HF)$ where HF is the Healing Function. The HF will be considered as dependent on the stress level applied and the healing rate η ; its value increases until a threshold stress value called critical stress σ_c , and for stress values higher than σ_c the value of HF starts decreasing.

258

259

According to the literature, following tendon injury, early mobilisation during the initial post-operative period accelerates the healing process. Specifically, low loads applied

260 during passive rehabilitation protocols facilitate tissue remodelling. However, active
 261 rehabilitation protocols involving higher loads have been shown to yield the best results in
 262 terms of mechanical properties and collagen turnover [9], [42], [43], [44]. Nevertheless, this
 263 enhancement of the healing effect persists only until a certain critical stress is reached,
 264 beyond which the healing effect of the tendon diminishes due to the formation of a gap
 265 between the tendon stumps [45]. Although the critical stress σ_c is not known, in this paper
 266 it has been assumed to reach the value of 0.5 times the ultimate tensile strength (UTS) to
 267 encompass the range of stresses developed during active motion. This is based on the
 268 observation that the stresses present in the Achilles Tendon during running activities are
 269 approximately 55 MPa, with the UTS being around 110 MPa [46], [47].

270 Therefore, it has been hypothesised that the *HF* exhibits a polynomial trend over the
 271 course of the tendon life cycles. The chosen polynomial equation is reported in equation 15,
 272 where x is the difference between the experimental maximum stress at each level and the
 273 critical stress $\sigma_{exp} - \sigma_c$ divided by the value of the critical stress that in this study was set as
 274 $\sigma_c = 0.5 UTS$ (see equation 16). Meanwhile the value of the healing rate η may vary within
 275 the range [0 – 0.6] as reported by Bosia et al. [30]. Figure 2 reports the graph for the Healing
 276 function. For the introduction of the HF, equation (11) was considered: here, the expression
 277 of the generalised stress intensity factor K_{NL}^* was modified to the healing generalised stress
 278 intensity factor \widehat{K}_{NL}^* , and specifically the expression of half crack size a was replaced by
 279 $a(1 - HF)$ as shown in equation 17.

280

$$HF = 0.1\eta x^3 - 1.1\eta x^2 + \eta \quad (15)$$

$$x = \frac{\sigma_{exp} - \sigma_c}{\sigma_c} \quad (16)$$

$$\widehat{K}_{NL}^* = Y\sigma(\pi a(1 - HF))^\alpha \quad (17)$$

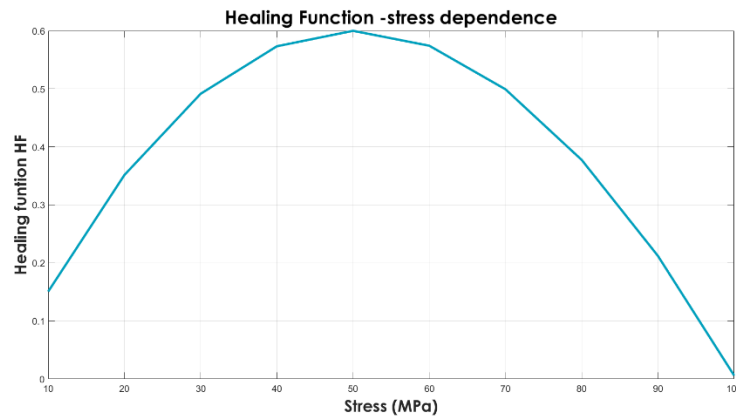


Figure 2: Healing Function for $\eta = 0.6$.

281

282

283 5. Monte Carlo analysis.

284 When addressing the evaluation of mechanical properties in biological materials, several
 285 challenges arise due to the considerable variability among samples. This variability
 286 stems from factors such as differences in the site of harvesting, variations between
 287 animal models, and diverse experimental setups, protocols, and animal handling
 288 practices. The types of variability encountered in animal models can be categorised into
 289 three groups: i) variability introduced by the experimenter, ii) inherent variability of the
 290 specimens, and iii) induced variabilities (i.e. variations resulting from the interaction
 291 between inherent differences among samples or individuals and external factors
 292 associated with experimental protocols or sample handling) [42]. Consequently, working
 293 with biological tissues inherently involves uncertainties and parameter variability [43].
 294 In light of these challenges, Monte Carlo (MC) analysis proves invaluable, as it allows to
 295 take into account uncertainties by using probabilistic distributions to represent variables
 296 and parameters, enabling the prediction of realistic outcomes. This method effectively
 297 accommodates both small and large uncertainties and captures partial correlations
 298 among different variables and parameters [44].

299 MC analysis stands out as one of the most widely employed methods for analysing
 300 uncertainties across various fields. It finds application in scenarios characterised by a
 301 certain degree of uncertainty, such as determining the elastic properties in carbon fibre
 302 composites [45], identifying viscoelastic properties through elastography [46], and
 303 assessing the impact of alterations in moment arms and muscle-tendon properties on
 304 the accuracy of predictions in muscle function models [47].

305 To comprehensively integrate the proposed GPE law and MC analysis, this section also
 306 explores the GPE equation in its inverse form. The numerical integration employed a

307 forward Euler explicit recursion method implemented within the MATLAB
308 environment. The experimental data used in this study are derived from EDL tendons
309 [22], where the authors measured the number of cycles for each of the 90 samples under
310 investigation, with 10 samples for each applied stress level. Given the absence of specific
311 guidance on probability distributions for GPE approach parameters, an initial
312 consideration of a uniform distribution was made. Subsequently, for comparison
313 purposes, a normal distribution was adopted.

314 In both cases, the mean values for parameters m_p and C were set to the values obtained
315 from the GA, i.e., $m_{best\ fit}$ and $C_{best\ fit}$. The MC simulation assumes statistical
316 independence of the parameters.

317 A number of 10000 sample runs of the integration were conducted in order to obtain an
318 accuracy in the range of two decimal places, as the accuracy of MC analysis is determined
319 by $(1/\sqrt{S})$, S being the number of samples. In particular, for the first analysis considering
320 a uniform distribution, the parameter m_p was assumed to vary within the values
321 $[m_{best\ fit} \pm 0.2m_{best\ fit}]$, and the parameter C ($\text{MPa}^{-m_p} \text{m}^{m_p/2+1}$) between $[C_{best\ fit} \pm$
322 $0.2C_{best\ fit}]$, meanwhile the value of the critical stress intensity factor K_{IC} ($\text{MPa}\sqrt{\text{m}}$) was
323 introduced considering the results from the GA $K_{IC\ best\ fit}$. In the second analysis a
324 normal distribution was considered, in which the parameter m_p was described by a mean
325 of $m_{best\ fit}$ and a standard deviation of $m_{best\ fit} * 0.2$, while the parameter C was
326 described by a mean of $C_{best\ fit}$ and a standard deviation of $C_{best\ fit} * 0.2$.

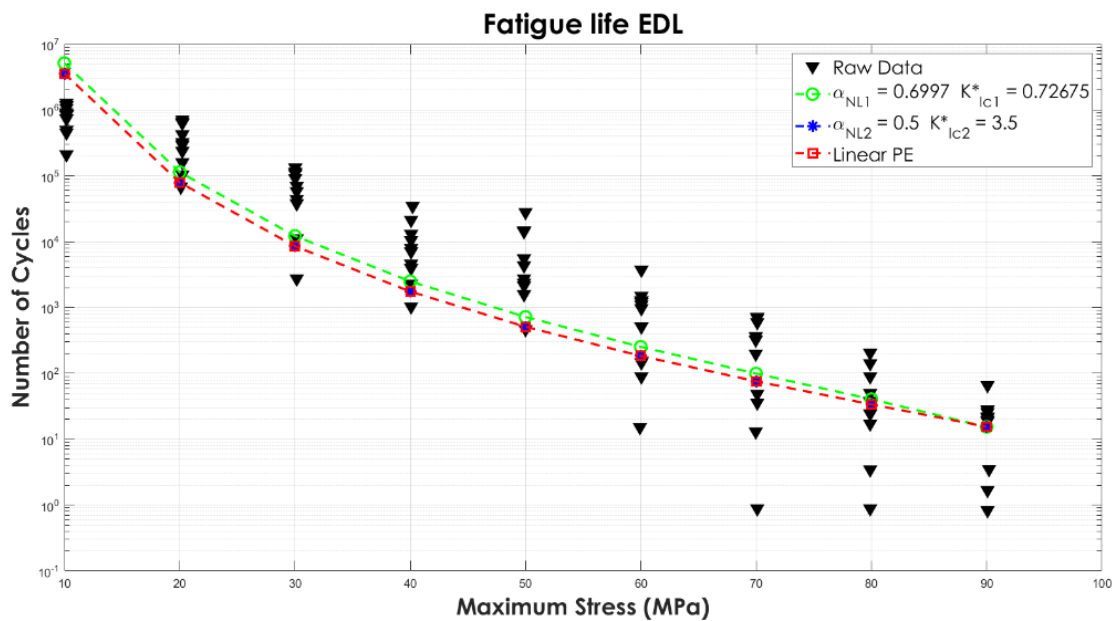
327 The range of the uniform distribution and the value of the standard deviation for the
328 normal distribution were chosen to adequately capture the variability of the
329 experimental data used in this study. This choice aligns with typical ranges observed in
330 biological tissue measurements [49].

331 6. Results and discussion.

332 6.1. Integration of the Generalised Paris- Erdogan law for non-linear materials

333 Figure 3 shows the curves obtained by the integration of the GEP law employing the
334 results from the GA, here listed: $m_{best\ fit} = 5.5$, $K_{IC\ best\ fit} = 3.5 \text{ MPa}\sqrt{\text{m}}$, $C_{best\ fit} =$
335 $3 * 10^{-5} \text{ MPa}^{-m_p} \text{m}^{m_p/2+1}$. The number of cycles in this graph and in the following figures
336 is intended as the number of cycles after which failure occurs for the different stress
337 levels. For comparison purposes, the traditional Paris-Erdogan (PE) law was integrated
338 using results from the Genetic Algorithm (GA). Additionally, in the integration of the

339 Generalised Paris-Erdogan (GPE) law, the parameter $\alpha = 0.5$, was also considered, as in
 340 this case the expression of the GPE law coincides with the traditional PE law. In figures
 341 3 and 4 the results corresponding to the GPE law for $\alpha = 0.7$ are shown in green, while
 342 the blue lines represent curves obtained for $\alpha = 0.5$, and the red curves represent the
 343 values obtained by integrating the traditional PE law. The values obtained for the
 344 generalised critical SIF are also reported in the graph legend, being $K_{IC}^* =$
 345 $0.73 \text{ MPa m}^{0.7}$, in case of $\alpha = 0.7$ and $K_{IC}^* = 3.5 \text{ MPa m}^{0.5}$ for $\alpha = 0.5$ that coincides with
 346 the value of the critical stress intensity factor obtained by the GA.



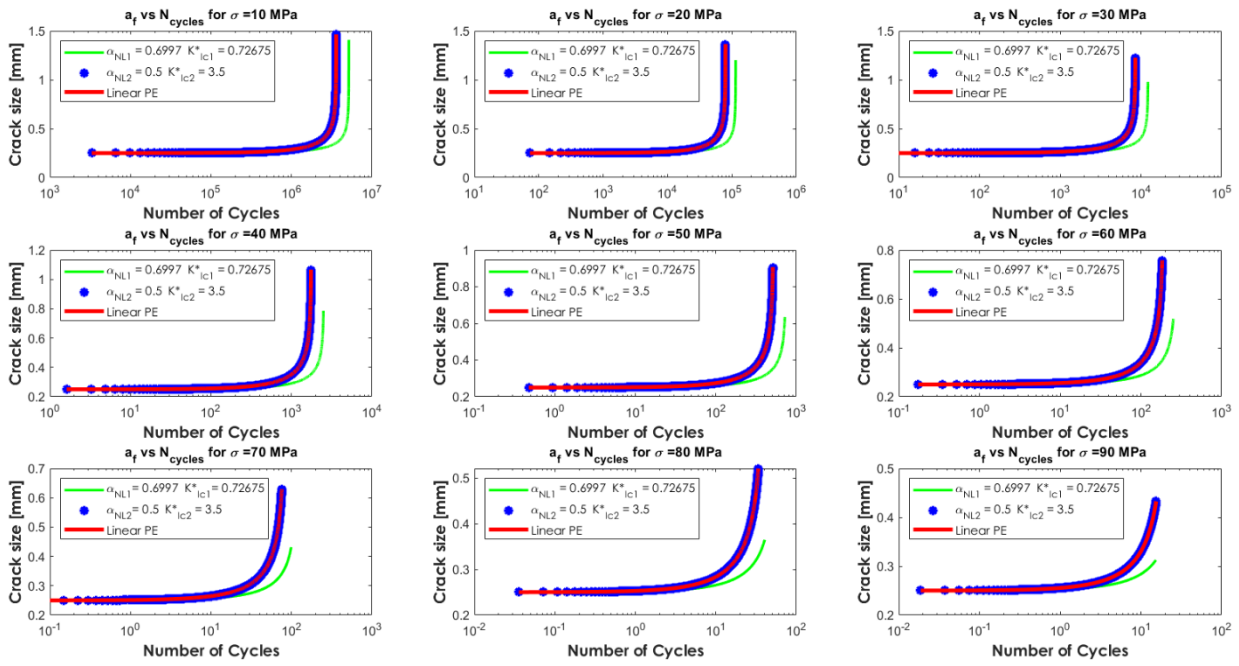
347
 348 *Figure 3: Fatigue life of EDL tendons considering GPE and traditional PE law, for the value of $\alpha = 0.5$ the GPE and the linear PE lines*
 349 *are superimposed, where the units of K_{IC}^* are $[\text{MPa m}^\alpha]$.*

350 According to Figure 3, it is evident that the number of cycles obtained for the GPE and
 351 linear PE law exhibits slight variations. Particularly, at lower stress levels, the variation
 352 is more pronounced compared to the values obtained at a stress level of 90 MPa.
 353 Furthermore, the values obtained for the lowest stress levels show an ineffective fit of
 354 the experimental data, leading to an overestimation in both cases.

355 From the integration of the GPE and linear PE law, it is possible to analyse the crack
 356 growth over the number of cycles for different max. stress values. Figure 4 displays the
 357 crack growth curves for all stress values in the experimental dataset. Observing the
 358 results, it stands out that the final crack size is smaller in the case of the GPE compared
 359 to the linear PE approach. In particular, the difference between the final crack size
 360 reached for the GPE and PE approaches is almost negligible at the stress value of 10
 361 MPa. However, for higher stress values, the final crack size difference increases
 362 consistently as the stress value increases. Notably, the final crack size always remains

363
364
365
366

smaller in the GPE non-linear approach compared to the linear PE one. Figure 3 also reveals that, for the GPE approach, the number of cycles is higher than the linear PE approach, except for the values of 90 MPa, where both approaches yield nearly the same number of cycles.



367
368
369

Figure 4: Crack size growth for the different stress values for the non-linear GPE and linear PE approach, where the units of K_{lc}^* are $[MPa m^\alpha]$.

370 *6.2. Healing function influence on the number of cycles*

371 Figure 5 illustrates the impact of applying the healing function on the number of cycles
372 obtained for the GPE approach with $\alpha=0.7$. It is evident that the number of cycles increases
373 with the different stress levels up to the critical stress value σ_c , where the value of the healing
374 function (HF) reaches its maximum (HF= η). The incorporation of the HF leads to a more
375 accurate fit of the experimental data within the stress range of 20-80 MPa. Additionally, it
376 is noteworthy that as the value of η increases, the number of cycles also increases
377 proportionally. However, for stress values of 10 and 90 MPa, there is not a significant change
378 in the number of cycles, as expected from the HF. It is important to highlight that no specific
379 considerations can be drawn regarding the long-term effects of the healing application, given
380 the absence of experimental in vivo data.

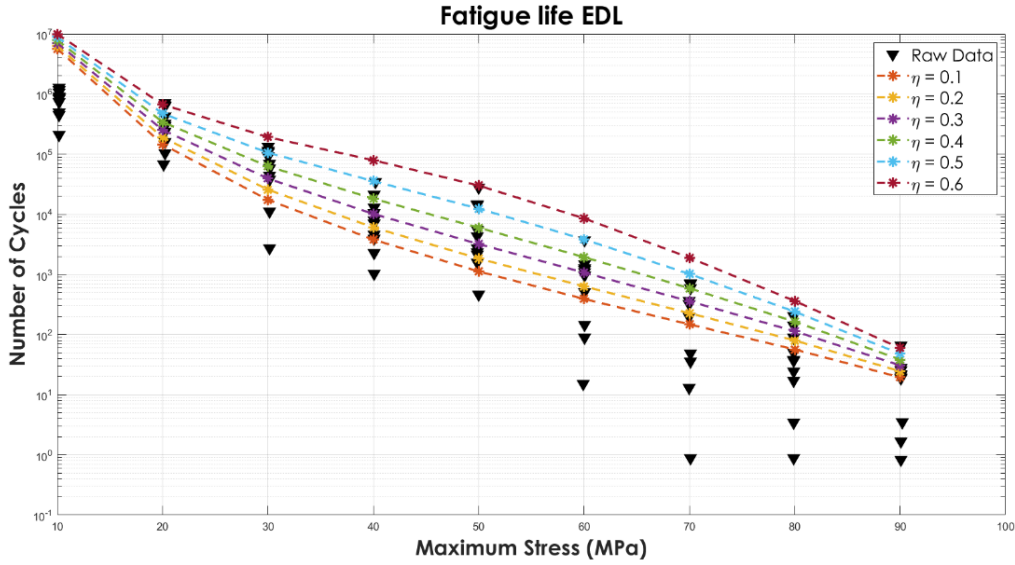


Figure 5: Effect of the Healing function in the number of cycles for GPE approach.

6.3. GPE for non-linear materials Monte Carlo analysis.

The results of the MC analysis are presented in Figure 6 for the GPE approach for the value of $\alpha = 0.7$ in case of a uniform distribution for the parameters m_p and C . In particular, the graph illustrates the substantial impact of introducing an uncertainty of 20% in only two parameters $C_{best\ fit}$ and $m_{best\ fit}$, which entails a significant change in the results. It is noticeable that the bounds amplitude is wider for lower and higher stress levels. Meanwhile, in correspondence to the stress values of 30-40 MPa, the bounds exhibit the narrowest amplitude. It has been observed that the tightest bounds consistently occur at 30-40 MPa for different values of α . Although most of the experimental points are within the bounds, there are some outliers. Specifically, those corresponding to stress values within the range of 20-50 MPa, where the interval for the number of cycles becomes narrower. The statistics for the first Monte Carlo simulation are shown in Table 2, where LogN is the logarithm of the number of cycles for the different stress values.

Table 2: Statistics for the logarithm of the number of cycles (Log N) of first Monte Carlo simulation, C and m_p have uniform distributions.

Statistics for LogN									
Stress [MPa]	10	20	30	40	50	60	70	80	90
Mean	6.84	5.09	4.10	3.41	2.88	2.44	2.04	1.67	1.26
Std. dv.	6.70	4.60	3.20	2.66	2.34	2.02	1.71	1.38	1.00
Min	6.09	4.76	3.99	3.23	2.58	2.05	1.58	1.15	0.69
Max	7.36	5.38	4.22	3.60	3.16	2.78	2.43	2.09	1.70

381

382

383

384

385

386

387

388

389

390

391

392

393

394

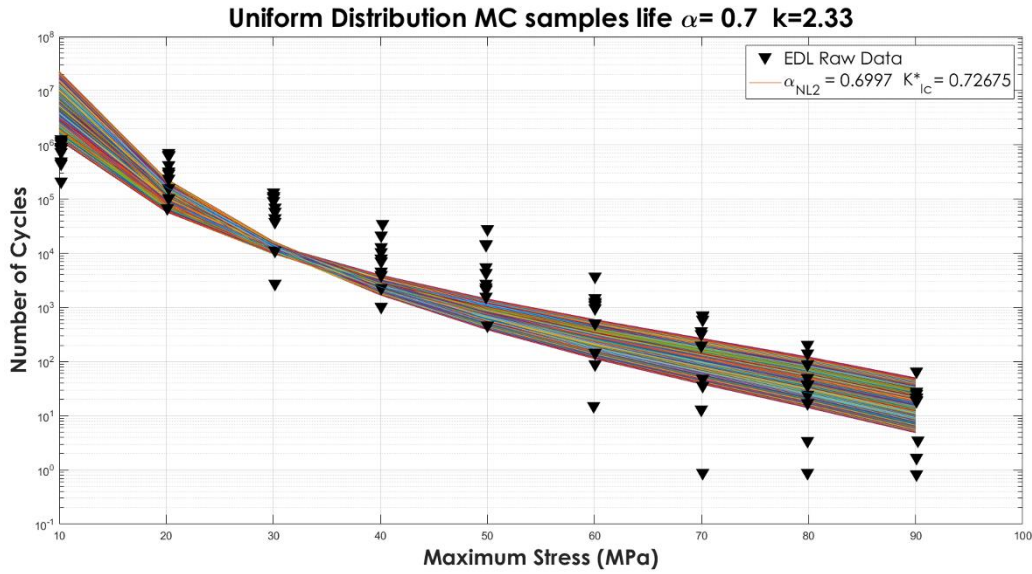
395

396

397

398

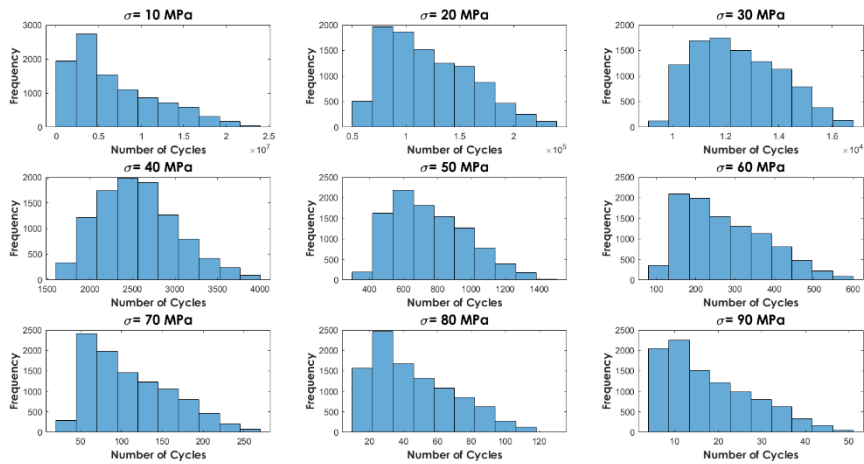
399



400

401 *Figure 6: Number of cycles obtained by Monte Carlo Analysis for the GPE approach with uniform distribution of m_p and C , where the*
 402 *units of K_{lc}^* are $[MPa m^\alpha]$.*

403 Figure 7 displays the diverse distributions of the number of cycles obtained for various stress
 404 values. For almost all stress values, the observed number of cycles exhibits similar
 405 distributions. However, a quasi-normal distribution shape is observed only in the case of
 406 stress values at 30 and 40 MPa, where the bounds are narrower.



407

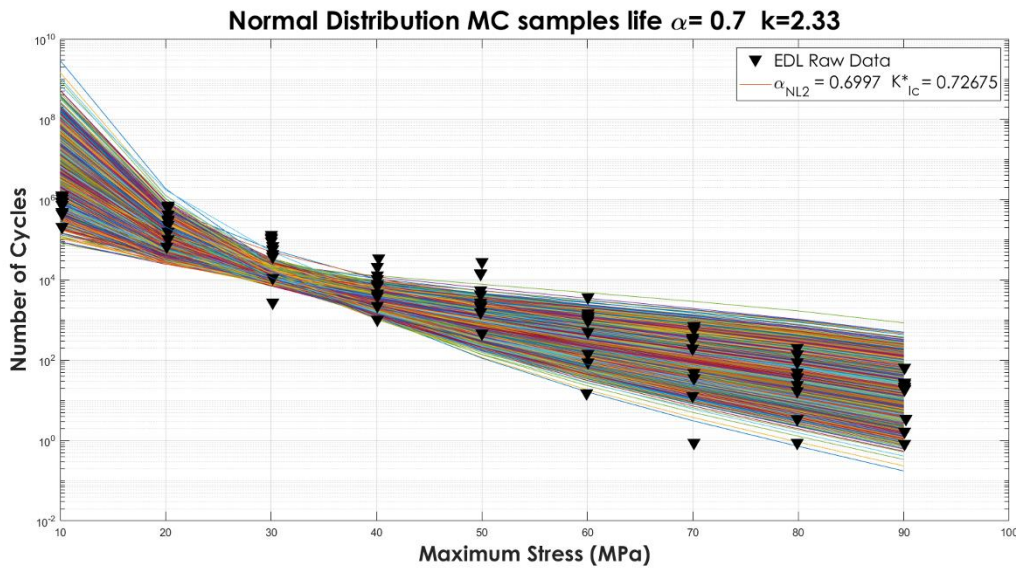
408 *Figure 7: Distributions of the number of cycles obtained with 10000 samples run for the different stress values.*

409 Figure 8 displays the number of cycles obtained for the second case Monte Carlo analysis,
 410 where the values of m_p and C follow a normal distribution. In this scenario, introducing
 411 a standard deviation of 20% of the mean value results in a greater dispersion of the
 412 obtained cycles. Notably, almost all experimental data are covered by the Monte Carlo
 413 simulation results in this analysis. It is worth mentioning that, similarly to the first

414 analysis, the narrowest section of the bounds corresponds to stress levels of 30-40 MPa.
 415 Table 3 presents the statistics for the second Monte Carlo simulation.

416 *Table 3: Statistics for the logarithm of the number of cycles (Log N) for the second Monte Carlo simulation.*

Statistics for LogN									
Stress [MPa]	10	20	30	40	50	60	70	80	90
Mean	7.09	5.14	4.12	3.44	2.94	2.52	2.16	1.81	1.42
Std. dv.	7.42	4.96	3.52	2.99	2.71	2.43	2.17	1.88	1.55
Min	4.82	4.35	3.83	2.96	2.12	1.42	0.83	0.29	0.26
Max	8.82	6.11	4.72	4.23	4.03	3.84	3.63	3.40	3.11



417
 418 *Figure 8: Number of cycles obtained by Monte Carlo Analysis for the GPE approach with normal distribution of m_p and C , where the*
 419 *units of K_{IC}^* are $[MPa m^\alpha]$.*

420 The distributions for the number of cycles at each stress level are depicted in Figure 9. In
 421 contrast to the previous distributions, in this case, with the same quantity of groups (10 for
 422 the histogram), it is evident that almost all values are concentrated in two or three classes
 423 out of 10. The uniform distribution results in a broader range of cycle values compared to
 424 the previous case. However, it is noteworthy that values with high frequency coincide with
 425 those obtained under the uniform distribution.

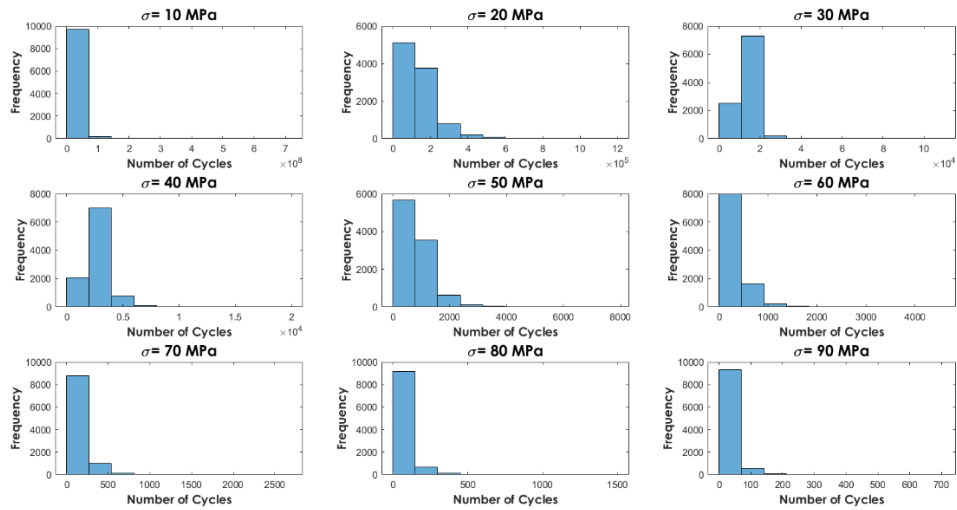


Figure 9: Distributions of the number of cycles obtained with 10000 samples runs for the different stress values.

6.4. Conclusions

The proposed generalisation of the Paris-Erdogan law for non-linear materials suggests that incorporating non-linearities into the Paris-Erdogan law designed for linear elastic materials does not yield significant improvements in terms of fitting experimental data, at least based on the examined case study. This leads to the consideration that, even though the Paris-Erdogan law was originally formulated for linear elastic materials, it may also find applicability for non-linear materials with a constitutive law analogous to that of the biological material constituting tendons. However, further investigation on this aspect is necessary, ideally with additional experimental data from specimens of various materials characterised by a non-linear polynomial constitutive law.

In this study, the mechanical parameters C and m_p for the PE law have been estimated in the case of tendons. Further studies are necessary to effectively validate these values. The introduction of the HF allows to observe an increase of the number of cycles for each stress value. This was expected, as self-healing is present in natural structures as a consequence of evolution and allows to repair the micro damages induced by physiological loads. However, additional investigations are needed to assess the hypothesis of the healing function's dependence on the stress levels as the most suitable representation for the healing process. The high variability among the samples, and their related mechanical and fatigue properties, allows to obtain reasonable bounds for a uniform distribution for the parameters for the GPE approach. In particular, it was observed that the Generalised Paris-Erdogan (GPE) approach exhibits high sensitivity to changes in input parameters under high and low stress conditions compared to medium stresses. This underscores the necessity for a comprehensive understanding of the model's behaviour under different stress conditions,

451 emphasising the need for further research to refine and validate the proposed approach in
452 various scenarios.

453 **Acknowledgments:** The authors express their gratitude to Dr. Rinto Roy and Mr. Vito
454 Burgio for their valuable suggestions and support.

455 7. **Bibliography**

- 456 [1] F. Fang and S. P. Lake, "Modelling approaches for evaluating multiscale tendon mechanics," *Interface*
457 *Focus*, vol. 6, no. 1. Royal Society of London, Feb. 06, 2016. doi: 10.1098/rsfs.2015.0044.
- 458 [2] R. F. Ker, "Dynamic tensile properties of the plantaris tendon of sheep (*Ovis Aries*)," 1981.
- 459 [3] H. R. C. Screen, "Hierarchical approaches to understanding tendon mechanics," *Journal of*
460 *Biomechanical Science and Engineering*, vol. 4, no. 4. pp. 481–499, 2009. doi: 10.1299/jbse.4.481.
- 461 [4] A. A. Biewener, "Tendons and Ligaments: Structure, Mechanical Behavior and Biological Function," in
462 *Collagen*, 2008, pp. 269–284.
- 463 [5] G. A. Lichtwark and A. M. Wilson, "In vivo mechanical properties of the human Achilles tendon
464 during one-legged hopping," *Journal of Experimental Biology*, vol. 208, no. 24, pp. 4715–4725, Dec.
465 2005, doi: 10.1242/jeb.01950.
- 466 [6] J. H. C. Wang, "Mechanobiology of tendon," *Journal of Biomechanics*, vol. 39, no. 9. pp. 1563–1582,
467 2006. doi: 10.1016/j.jbiomech.2005.05.011.
- 468 [7] J. H. Shepherd and H. R. C. Screen, "Fatigue loading of tendon," *International Journal of Experimental*
469 *Pathology*, vol. 94, no. 4. pp. 260–270, Aug. 2013. doi: 10.1111/iep.12037.
- 470 [8] U. Giuseppe Longo, M. Ronga, and N. Maffulli, "Achilles Tendinopathy," 2009. [Online]. Available:
471 www.sportsmedarthro.com
- 472 [9] N. Maffulli, U. G. Longo, A. Kadakia, and F. Spiezia, "Achilles tendinopathy," *Foot and Ankle Surgery*,
473 vol. 26, no. 3. Elsevier Ltd, pp. 240–249, Apr. 01, 2020. doi: 10.1016/j.fas.2019.03.009.
- 474 [10] M. I. Boyer, C. A. Goldfarb, and R. H. Gelberman, "Recent progress in flexor tendon healing: The
475 modulation of tendon healing with rehabilitation variables," *Journal of Hand Therapy*, vol. 18, no. 2,
476 pp. 80–85, 2005, doi: 10.1197/j.jht.2005.01.009.
- 477 [11] J. D. Urschel, P. G. Scottand, and H. T. G. Williams, "The effect of mechanical stress on soft and hard
478 tissue repair; a review," *British Journal of Plastic Surgery*, vol. 41, pp. 182–186, 1988.
- 479 [12] C. Martin and W. Sun, "Fatigue Damage of Collagenous Tissues: Experiment, Modeling and
480 Simulation Studies," *J Long Term Eff Med Implants.*, vol. 25, pp. 55–73, 2015.
- 481 [13] X. T. Wang and R. F. Ker, "Fatigue rupture of wallaby tail tendons," *J Exp Biol*, vol. 198, pp. 847–852,
482 1995.
- 483 [14] R. F. Ker, X. T. Wang, and A. V. L. Pike, "Fatigue quality of mammalian tendons," *J Exp Biol*, vol. 203,
484 pp. 1317–1327, 2000.
- 485 [15] K. Pedaprolu and S. E. Szczesny, "A Novel, Open-Source, Low-Cost Bioreactor for Load-Controlled
486 Cyclic Loading of Tendon Explants," *J Biomech Eng*, vol. 144, no. 8, Aug. 2022, doi:
487 10.1115/1.4053795.
- 488 [16] D. T. Fung *et al.*, "Subrupture tendon fatigue damage," *Journal of Orthopaedic Research*, vol. 27, no.
489 2, pp. 264–273, Feb. 2009, doi: 10.1002/jor.20722.
- 490 [17] L. J. Soslowsky *et al.*, "Overuse activity injures the supraspinatus tendon in an animal model: A
491 histologic and biomechanical study," *J Shoulder Elbow Surg*, vol. 9, no. 2, pp. 79–84, 2000, doi:
492 10.1067/mse.2000.101962.

- 493 [18] A. Scott, J. L. Cook, D. A. Hart, D. C. Walker, V. Duronio, and K. M. Khan, "Tenocyte Responses to
494 Mechanical Loading In Vivo," *Arthritis Rheum*, vol. 56, no. 3, pp. 871–881, Mar. 2007, doi:
495 10.1002/art.22446.
- 496 [19] D. T. Fung *et al.*, "Early response to tendon fatigue damage accumulation in a novel in vivo model," *J*
497 *Biomech*, vol. 43, no. 2, pp. 274–279, Jan. 2010, doi: 10.1016/j.jbiomech.2009.08.039.
- 498 [20] N. Andarawis-Puri and E. L. Flatow, "Tendon fatigue in response to mechanical loading," *J*
499 *Musculoskelet Neuronal Interact*, vol. 11, no. 2, pp. 106–114, 2011.
- 500 [21] J. B. Sereysky, N. Andarawis-Puri, K. J. Jepsen, and E. L. Flatow, "Structural and mechanical effects of
501 in vivo fatigue damage induction on murine tendon," *Journal of Orthopaedic Research*, vol. 30, no. 6,
502 pp. 965–972, Jun. 2012, doi: 10.1002/jor.22012.
- 503 [22] H. Schechtman and D. L. Bader, "In vitro fatigue of human tendons," *J Biomech*, vol. 30, no. 8, pp.
504 829–835, 1997.
- 505 [23] T. A. L. Wren, D. P. Lindsey, G. S. Beaupré, and D. R. Carter, "Effects of creep and cyclic loading on the
506 mechanical properties and failure of human Achilles tendons," *Ann Biomed Eng*, vol. 31, no. 6, pp.
507 710–717, 2003, doi: 10.1114/1.1569267.
- 508 [24] C. R. Firminger and W. B. Edwards, "Effects of cyclic loading on the mechanical properties and failure
509 of human patellar tendon," *J Biomech*, vol. 120, May 2021, doi: 10.1016/j.jbiomech.2021.110345.
- 510 [25] B. R. Freedman, J. J. Sarver, M. R. Buckley, P. B. Voleti, and L. J. Soslowsky, "Biomechanical and
511 structural response of healing Achilles tendon to fatigue loading following acute injury," *J Biomech*,
512 vol. 47, no. 9, pp. 2028–2034, Jun. 2014, doi: 10.1016/j.jbiomech.2013.10.054.
- 513 [26] T. W. Herod, N. C. Chambers, and S. P. Veres, "Collagen fibrils in functionally distinct tendons have
514 differing structural responses to tendon rupture and fatigue loading," *Acta Biomater*, vol. 42, pp.
515 296–307, Sep. 2016, doi: 10.1016/j.actbio.2016.06.017.
- 516 [27] J. Gregory, A. L. Hazel, and T. Shearer, "A microstructural model of tendon failure," *J Mech Behav*
517 *Biomed Mater*, vol. 122, Oct. 2021, doi: 10.1016/j.jmbbm.2021.104665.
- 518 [28] K. Linka, M. Hillgärtner, and M. Itskov, "Fatigue of soft fibrous tissues: Multi-scale mechanics and
519 constitutive modeling," *Acta Biomater*, vol. 71, pp. 398–410, Apr. 2018, doi:
520 10.1016/j.actbio.2018.03.010.
- 521 [29] C. Martin and W. Sun, "Simulation of long-term fatigue damage in bioprosthetic heart valves: Effects
522 of leaflet and stent elastic properties," *Biomech Model Mechanobiol*, vol. 13, no. 4, pp. 759–770,
523 2014, doi: 10.1007/s10237-013-0532-x.
- 524 [30] F. Bosia, M. Merlino, and N. M. Pugno, "Fatigue of self-healing hierarchical soft nanomaterials: The
525 case study of the tendon in sportsmen," *J Mater Res*, vol. 30, no. 1, pp. 2–9, Sep. 2014, doi:
526 10.1557/jmr.2014.335.
- 527 [31] S. M. Adeeb, M. L. Zec, G. M. Thornton, C. B. Frank, and N. G. Shrive, "A novel application of the
528 principles of Linear Elastic Fracture Mechanics (LEFM) to the fatigue behavior of tendon tissue," *J*
529 *Biomech Eng*, vol. 126, no. 5, pp. 641–650, Oct. 2004, doi: 10.1115/1.1800556.
- 530 [32] S. H. Hosseini Nasab *et al.*, "Uncertainty in Muscle–Tendon Parameters can Greatly Influence the
531 Accuracy of Knee Contact Force Estimates of Musculoskeletal Models," *Front Bioeng Biotechnol*, vol.
532 10, Jun. 2022, doi: 10.3389/fbioe.2022.808027.

- 533 [33] D. Balzani, T. Schmidt, and M. Ortiz, "Method for the quantification of rupture probability in soft
534 collagenous tissues," *Int J Numer Method Biomed Eng*, vol. 33, no. 1, Jan. 2017, doi:
535 10.1002/cnm.2781.
- 536 [34] J. Haughton, S. L. Cotter, W. J. Parnell, and T. Shearer, "Bayesian inference on a microstructural,
537 hyperelastic model of tendon deformation," *J R Soc Interface*, vol. 19, no. 190, 2022, doi:
538 10.1098/rsif.2022.0031.
- 539 [35] K. Worden and G. Manson, "Prognosis under uncertainty-An idealised computational case study,"
540 2008.
- 541 [36] C. Surace and K. Worden, "Extended Analysis of a Damage Prognosis Approach Based on Interval
542 Arithmetic," *Strain*, vol. 47, no. 6, pp. 544–554, Dec. 2011, doi: 10.1111/j.1475-1305.2011.00815.x.
- 543 [37] A. Carpinteri and N. Pugno, "Cracks and re-entrant corners in functionally graded materials," *Eng
544 Fract Mech*, vol. 73, no. 10, pp. 1279–1291, Jul. 2006, doi: 10.1016/j.engfracmech.2006.01.008.
- 545 [38] N. Pugno, A. Carpinteri, M. Ippolito, A. Mattoni, and L. Colombo, "Atomistic fracture: QFM vs. MD,"
546 *Eng Fract Mech*, vol. 75, no. 7, pp. 1794–1803, May 2008, doi: 10.1016/j.engfracmech.2007.01.028.
- 547 [39] G. A. Von Forell, P. S. Hyung, and A. E. Bowden, "Failure modes and fracture toughness in partially
548 torn ligaments and tendons," *J Mech Behav Biomed Mater*, vol. 35, pp. 77–84, 2014, doi:
549 10.1016/j.jmbbm.2014.03.020.
- 550 [40] D. Taylor, N. O'Mara, E. Ryan, M. Takaza, and C. Simms, "The fracture toughness of soft tissues," *J
551 Mech Behav Biomed Mater*, vol. 6, pp. 139–147, Feb. 2012, doi: 10.1016/j.jmbbm.2011.09.018.
- 552 [41] J. R. Rice and G. F. Rosengren, "Plane strain deformation near a crack tip in a power-law hardening
553 material," Pergamon Press, 1968.
- 554 [42] B. R. Howard, "Control of Variability," *ILAR J.*, vol. 43, no. 4, pp. 194–201, 2002, [Online]. Available:
555 <https://academic.oup.com/ilarjournal/article/43/4/194/981669>
- 556 [43] J. F. Weber, A. M. R. Agur, A. Y. Fattah, K. D. Gordon, and M. L. Oliver, "Tensile mechanical properties
557 of human forearm tendons," *Journal of Hand Surgery: European Volume*, vol. 40, no. 7, pp. 711–719,
558 Sep. 2015, doi: 10.1177/1753193415584715.
- 559 [44] C. E. Papadopoulos and H. Yeung, "Uncertainty estimation and Monte Carlo simulation method,"
560 2001. [Online]. Available: www.elsevier.com/locate/flowmeasinst
- 561 [45] M. Shan, L. Zhao, and J. Ye, "A Novel Micromechanics-Model-Based Probabilistic Analysis Method for
562 the Elastic Properties of Unidirectional CFRP Composites," *Materials*, vol. 15, no. 15, Aug. 2022, doi:
563 10.3390/ma15155090.
- 564 [46] E. Van Houten, G. Geymonat, F. Krasucki, and B. Wattrisse, "General guidelines for the performance
565 of viscoelastic property identification in elastography: A Monte-Carlo analysis from a closed-form
566 solution," *Int J Numer Method Biomed Eng*, vol. 39, no. 8, Aug. 2023, doi: 10.1002/cnm.3741.
- 567 [47] D. C. Ackland, Y. C. Lin, and M. G. Pandy, "Sensitivity of model predictions of muscle function to
568 changes in moment arms and muscle-tendon properties: A Monte-Carlo analysis," *J Biomech*, vol. 45,
569 no. 8, pp. 1463–1471, May 2012, doi: 10.1016/j.jbiomech.2012.02.023.

570

571

- 572 [1] F. Fang and S. P. Lake, "Modelling approaches for evaluating multiscale tendon mechanics," *Interface*
573 *Focus*, vol. 6, no. 1. Royal Society of London, Feb. 06, 2016. doi: 10.1098/rsfs.2015.0044.
- 574 [2] R. F. Ker, "Dynamic tensile properties of the plantaris tendon of sheep (*Ovis Aries*)," 1981.
- 575 [3] H. R. C. Screen, "Hierarchical approaches to understanding tendon mechanics," *Journal of*
576 *Biomechanical Science and Engineering*, vol. 4, no. 4. pp. 481–499, 2009. doi: 10.1299/jbse.4.481.
- 577 [4] A. A. Biewener, "Tendons and Ligaments: Structure, Mechanical Behavior and Biological Function," in
578 *Collagen*, 2008, pp. 269–284.
- 579 [5] G. A. Lichtwark and A. M. Wilson, "In vivo mechanical properties of the human Achilles tendon
580 during one-legged hopping," *Journal of Experimental Biology*, vol. 208, no. 24, pp. 4715–4725, Dec.
581 2005, doi: 10.1242/jeb.01950.
- 582 [6] J. H. C. Wang, "Mechanobiology of tendon," *Journal of Biomechanics*, vol. 39, no. 9. pp. 1563–1582,
583 2006. doi: 10.1016/j.jbiomech.2005.05.011.
- 584 [7] J. H. Shepherd and H. R. C. Screen, "Fatigue loading of tendon," *International Journal of Experimental*
585 *Pathology*, vol. 94, no. 4. pp. 260–270, Aug. 2013. doi: 10.1111/iep.12037.
- 586 [8] U. Giuseppe Longo, M. Ronga, and N. Maffulli, "Achilles Tendinopathy," 2009. [Online]. Available:
587 www.sportsmedarthro.com
- 588 [9] N. Maffulli, U. G. Longo, A. Kadakia, and F. Spiezia, "Achilles tendinopathy," *Foot and Ankle Surgery*,
589 vol. 26, no. 3. Elsevier Ltd, pp. 240–249, Apr. 01, 2020. doi: 10.1016/j.fas.2019.03.009.
- 590 [10] M. I. Boyer, C. A. Goldfarb, and R. H. Gelberman, "Recent progress in flexor tendon healing: The
591 modulation of tendon healing with rehabilitation variables," *Journal of Hand Therapy*, vol. 18, no. 2,
592 pp. 80–85, 2005, doi: 10.1197/j.jht.2005.01.009.
- 593 [11] J. D. Urschel, P. G. Scottand, and H. T. G. Williams, "The effect of mechanical stress on soft and hard
594 tissue repair; a review," *British Journal of Plastic Surgery*, vol. 41, pp. 182–186, 1988.
- 595 [12] C. Martin and W. Sun, "Fatigue Damage of Collagenous Tissues: Experiment, Modeling and
596 Simulation Studies," *J Long Term Eff Med Implants.*, vol. 25, pp. 55–73, 2015.
- 597 [13] X. T. Wang and R. F. Ker, "Fatigue rupture of wallaby tail tendons," *J Exp Biol*, vol. 198, pp. 847–852,
598 1995.
- 599 [14] R. F. Ker, X. T. Wang, and A. V. L. Pike, "Fatigue quality of mammalian tendons," *J Exp Biol*, vol. 203,
600 pp. 1317–1327, 2000.
- 601 [15] K. Pedaprolu and S. E. Szczesny, "A Novel, Open-Source, Low-Cost Bioreactor for Load-Controlled
602 Cyclic Loading of Tendon Explants," *J Biomech Eng*, vol. 144, no. 8, Aug. 2022, doi:
603 10.1115/1.4053795.
- 604 [16] D. T. Fung *et al.*, "Subrupture tendon fatigue damage," *Journal of Orthopaedic Research*, vol. 27, no.
605 2, pp. 264–273, Feb. 2009, doi: 10.1002/jor.20722.
- 606 [17] L. J. Soslowsky *et al.*, "Overuse activity injures the supraspinatus tendon in an animal model: A
607 histologic and biomechanical study," *J Shoulder Elbow Surg*, vol. 9, no. 2, pp. 79–84, 2000, doi:
608 10.1067/mse.2000.101962.

- 609 [18] A. Scott, J. L. Cook, D. A. Hart, D. C. Walker, V. Duronio, and K. M. Khan, "Tenocyte Responses to
610 Mechanical Loading In Vivo," *Arthritis Rheum*, vol. 56, no. 3, pp. 871–881, Mar. 2007, doi:
611 10.1002/art.22446.
- 612 [19] D. T. Fung *et al.*, "Early response to tendon fatigue damage accumulation in a novel in vivo model," *J*
613 *Biomech*, vol. 43, no. 2, pp. 274–279, Jan. 2010, doi: 10.1016/j.jbiomech.2009.08.039.
- 614 [20] N. Andarawis-Puri and E. L. Flatow, "Tendon fatigue in response to mechanical loading," *J*
615 *Musculoskelet Neuronal Interact*, vol. 11, no. 2, pp. 106–114, 2011.
- 616 [21] J. B. Sereysky, N. Andarawis-Puri, K. J. Jepsen, and E. L. Flatow, "Structural and mechanical effects of
617 in vivo fatigue damage induction on murine tendon," *Journal of Orthopaedic Research*, vol. 30, no. 6,
618 pp. 965–972, Jun. 2012, doi: 10.1002/jor.22012.
- 619 [22] H. Schechtman and D. L. Bader, "In vitro fatigue of human tendons," *J Biomech*, vol. 30, no. 8, pp.
620 829–835, 1997.
- 621 [23] T. A. L. Wren, D. P. Lindsey, G. S. Beaupré, and D. R. Carter, "Effects of creep and cyclic loading on the
622 mechanical properties and failure of human Achilles tendons," *Ann Biomed Eng*, vol. 31, no. 6, pp.
623 710–717, 2003, doi: 10.1114/1.1569267.
- 624 [24] C. R. Firminger and W. B. Edwards, "Effects of cyclic loading on the mechanical properties and failure
625 of human patellar tendon," *J Biomech*, vol. 120, May 2021, doi: 10.1016/j.jbiomech.2021.110345.
- 626 [25] B. R. Freedman, J. J. Sarver, M. R. Buckley, P. B. Voleti, and L. J. Soslowsky, "Biomechanical and
627 structural response of healing Achilles tendon to fatigue loading following acute injury," *J Biomech*,
628 vol. 47, no. 9, pp. 2028–2034, Jun. 2014, doi: 10.1016/j.jbiomech.2013.10.054.
- 629 [26] T. W. Herod, N. C. Chambers, and S. P. Veres, "Collagen fibrils in functionally distinct tendons have
630 differing structural responses to tendon rupture and fatigue loading," *Acta Biomater*, vol. 42, pp.
631 296–307, Sep. 2016, doi: 10.1016/j.actbio.2016.06.017.
- 632 [27] J. Gregory, A. L. Hazel, and T. Shearer, "A microstructural model of tendon failure," *J Mech Behav*
633 *Biomed Mater*, vol. 122, Oct. 2021, doi: 10.1016/j.jmbbm.2021.104665.
- 634 [28] K. Linka, M. Hillgärtner, and M. Itskov, "Fatigue of soft fibrous tissues: Multi-scale mechanics and
635 constitutive modeling," *Acta Biomater*, vol. 71, pp. 398–410, Apr. 2018, doi:
636 10.1016/j.actbio.2018.03.010.
- 637 [29] C. Martin and W. Sun, "Simulation of long-term fatigue damage in bioprosthetic heart valves: Effects
638 of leaflet and stent elastic properties," *Biomech Model Mechanobiol*, vol. 13, no. 4, pp. 759–770,
639 2014, doi: 10.1007/s10237-013-0532-x.
- 640 [30] F. Bosia, M. Merlino, and N. M. Pugno, "Fatigue of self-healing hierarchical soft nanomaterials: The
641 case study of the tendon in sportsmen," *J Mater Res*, vol. 30, no. 1, pp. 2–9, Sep. 2014, doi:
642 10.1557/jmr.2014.335.
- 643 [31] S. M. Adeeb, M. L. Zec, G. M. Thornton, C. B. Frank, and N. G. Shrive, "A novel application of the
644 principles of Linear Elastic Fracture Mechanics (LEFM) to the fatigue behavior of tendon tissue," *J*
645 *Biomech Eng*, vol. 126, no. 5, pp. 641–650, Oct. 2004, doi: 10.1115/1.1800556.
- 646 [32] S. H. Hosseini Nasab *et al.*, "Uncertainty in Muscle–Tendon Parameters can Greatly Influence the
647 Accuracy of Knee Contact Force Estimates of Musculoskeletal Models," *Front Bioeng Biotechnol*, vol.
648 10, Jun. 2022, doi: 10.3389/fbioe.2022.808027.

- 649 [33] D. Balzani, T. Schmidt, and M. Ortiz, "Method for the quantification of rupture probability in soft
650 collagenous tissues," *Int J Numer Method Biomed Eng*, vol. 33, no. 1, Jan. 2017, doi:
651 10.1002/cnm.2781.
- 652 [34] J. Haughton, S. L. Cotter, W. J. Parnell, and T. Shearer, "Bayesian inference on a microstructural,
653 hyperelastic model of tendon deformation," *J R Soc Interface*, vol. 19, no. 190, 2022, doi:
654 10.1098/rsif.2022.0031.
- 655 [35] K. Worden and G. Manson, "Prognosis under uncertainty-An idealised computational case study,"
656 2008.
- 657 [36] C. Surace and K. Worden, "Extended Analysis of a Damage Prognosis Approach Based on Interval
658 Arithmetic," *Strain*, vol. 47, no. 6, pp. 544–554, Dec. 2011, doi: 10.1111/j.1475-1305.2011.00815.x.
- 659 [37] A. Carpinteri and N. Pugno, "Cracks and re-entrant corners in functionally graded materials," *Eng*
660 *Fract Mech*, vol. 73, no. 10, pp. 1279–1291, Jul. 2006, doi: 10.1016/j.engfracmech.2006.01.008.
- 661 [38] N. Pugno, A. Carpinteri, M. Ippolito, A. Mattoni, and L. Colombo, "Atomistic fracture: QFM vs. MD,"
662 *Eng Fract Mech*, vol. 75, no. 7, pp. 1794–1803, May 2008, doi: 10.1016/j.engfracmech.2007.01.028.
- 663 [39] G. A. Von Forell, P. S. Hyung, and A. E. Bowden, "Failure modes and fracture toughness in partially
664 torn ligaments and tendons," *J Mech Behav Biomed Mater*, vol. 35, pp. 77–84, 2014, doi:
665 10.1016/j.jmbbm.2014.03.020.
- 666 [40] D. Taylor, N. O'Mara, E. Ryan, M. Takaza, and C. Simms, "The fracture toughness of soft tissues," *J*
667 *Mech Behav Biomed Mater*, vol. 6, pp. 139–147, Feb. 2012, doi: 10.1016/j.jmbbm.2011.09.018.
- 668 [41] J. R. Rice and G. F. Rosengren, "Plane strain deformation near a crack tip in a power-law hardening
669 material," Pergamon Press, 1968.
- 670 [42] B. R. Howard, "Control of Variability," *ILAR J.*, vol. 43, no. 4, pp. 194–201, 2002, [Online]. Available:
671 <https://academic.oup.com/ilarjournal/article/43/4/194/981669>
- 672 [43] J. F. Weber, A. M. R. Agur, A. Y. Fattah, K. D. Gordon, and M. L. Oliver, "Tensile mechanical properties
673 of human forearm tendons," *Journal of Hand Surgery: European Volume*, vol. 40, no. 7, pp. 711–719,
674 Sep. 2015, doi: 10.1177/1753193415584715.
- 675 [44] C. E. Papadopoulos and H. Yeung, "Uncertainty estimation and Monte Carlo simulation method,"
676 2001. [Online]. Available: www.elsevier.com/locate/flowmeasinst
- 677 [45] M. Shan, L. Zhao, and J. Ye, "A Novel Micromechanics-Model-Based Probabilistic Analysis Method for
678 the Elastic Properties of Unidirectional CFRP Composites," *Materials*, vol. 15, no. 15, Aug. 2022, doi:
679 10.3390/ma15155090.
- 680 [46] E. Van Houten, G. Geymonat, F. Krasucki, and B. Wattrisse, "General guidelines for the performance
681 of viscoelastic property identification in elastography: A Monte-Carlo analysis from a closed-form
682 solution," *Int J Numer Method Biomed Eng*, vol. 39, no. 8, Aug. 2023, doi: 10.1002/cnm.3741.
- 683 [47] D. C. Ackland, Y. C. Lin, and M. G. Pandy, "Sensitivity of model predictions of muscle function to
684 changes in moment arms and muscle-tendon properties: A Monte-Carlo analysis," *J Biomech*, vol. 45,
685 no. 8, pp. 1463–1471, May 2012, doi: 10.1016/j.jbiomech.2012.02.023.